

Kondo behavior in the asymmetric Anderson model: Analytic approach

Václav Janiš* and Pavel Augustinský†

Institute of Physics, Academy of Sciences of the Czech Republic, Na Slovance 2, CZ-18221 Praha 8, Czech Republic

(Received 7 September 2007; published 8 February 2008)

The low-temperature behavior of the asymmetric single-impurity Anderson model is studied by diagrammatic methods resulting in analytically controllable approximations. We first discuss the ways one can simplify parquet equations in critical regions of singularities in the two-particle vertex. The scale vanishing at the critical point defines the Kondo temperature at which the electron-hole correlation function saturates. We show that a two-particle criticality exists at any filling of the impurity level. A quasiparticle resonance peak in the spectral function, however, forms only in almost electron-hole symmetric situations. We relate the Kondo temperature with the width of the resonance peak. Finally, we discuss the existence of satellite Hubbard bands in the spectral function.

DOI: [10.1103/PhysRevB.77.085106](https://doi.org/10.1103/PhysRevB.77.085106)

PACS number(s): 72.15.Qm, 75.20.Hr

I. INTRODUCTION

The single-impurity Anderson model (SIAM) has attracted much interest from theoretical physicists from its introduction in the early 1960s as a simple model for formation of local magnetic moments.¹ One of the reasons for the interest in SIAM has been its connection with the s - d exchange model and the Kondo effect² demonstrating a nontrivial strong-coupling behavior. The model won on importance after finding an exact solution with an algebraic Bethe ansatz.³ Revival of interests in reliable methods suitable for solving impurity models was brought with the concept of the dynamical mean-field theory of correlated lattice electrons.⁴ In particular, methods addressing dynamical properties of impurity models have been demanded in the mean-field description of strongly correlated systems. Since the exact algebraic approaches cover only static properties, a number of approximate analytic and numerical approaches have been revisited in the effort to provide an accurate impurity solver for strong electron correlations.

The direct way to treat the dynamics of SIAM is to use the perturbation theory in the interaction strength. It is known that such a perturbation series converges for all interaction strengths and second order already gives rather accurate results.^{5,6} Unrenormalized weak-coupling expansions break down in critical regions of any phase transition signaled by a singularity in a two-particle correlation function. Hence, extension of perturbative expansions to the strong-coupling regime of translationally invariant lattice models is questionable. There are renormalized perturbation expansions based either on multiple scatterings [fluctuation exchange, (FLEX)]⁷ or on low-frequency renormalizations of the Fermi-liquid parameters.⁸ The former approach does not reproduce the Kondo scale in SIAM and the latter fits for heavy Fermion systems but is not suitable for the description of critical instabilities of the Fermi-liquid state. On the other hand, strong-coupling expansions based on the infinite interaction model^{9,10} fail to reproduce the Fermi-liquid regime in the weak-coupling limit. A dynamical theory reliably describing the transition from the weak-coupling Fermi liquid to a strong-coupling solution is still missing. There exists an approximate scheme called local moment approach that ful-

fills a number of correct limits: weak-coupling Fermi liquid, atomic limit, and the Kondo regime.¹¹ This approximation resembles an alloy-analogy solution where the strong-coupling limit is plagued with a symmetry breaking and an unphysical static order (value of the local magnetic moment).

Presently, the most comprehensive quantitative approaches producing dynamical properties of the impurity models are quantum Monte Carlo¹² (QMC) and the numerical renormalization group (NRG).¹³ The latter scheme was first devised by Wilson when solving the s - d exchange model and later extended to SIAM in Ref. 14. Although designed for static thermodynamic properties, NRG can be used to some extent for the calculation of dynamical quantities as well.^{15,16} Since the quantum Monte Carlo is restricted to rather high temperatures, NRG represents the most accurate quantitative low-temperature and low-energy solution of impurity problems for intermediate couplings nowadays.¹⁷

Purely numerical schemes such as NRG and QMC deliver rather accurate results for nonsingular quantities. Their stability weakens and the convergence slows down apparently once we reach critical regions of singular points in static or dynamical (correlation) functions. The genuine critical behavior can then be deduced by either appropriately increasing the precision of the numerical scheme or indirectly via extrapolations. When no simple (power) scaling law holds we, however, cannot make *definite* conclusions on the existence and character of the critical behavior in the strong-coupling regime of correlated electrons. An analytic theory must then help us.

We recently developed an analytic approximate scheme summing selected classes of Feynman diagrams for the two-particle vertex.¹⁸ The approximation is justified in the critical region of the Bethe-Salpeter equation in the electron-hole scattering channel and uses a simplified version of the parquet equations for the electron-hole and electron-electron irreducible vertex functions. We demonstrated that in the symmetric case of SIAM, the low-energy Kondo scale is qualitatively correctly reproduced (universal features thereof) in this approximation.¹⁸

In this paper, we discuss the strong-coupling Kondo behavior in SIAM in a more general context beyond the symmetric case. For this purpose, we use simplified parquet equations. We introduce a general method of simplification

of the parquet equations for impurity models. It is based on a partial separation of short- and long-range energy scales inferred by a singularity in one of the Bethe-Salpeter equations for the two-particle vertex. Although this singularity is reached in SIAM only in the limit of infinite electron repulsion, its critical region extends deep into finite interaction strengths comparable with the width of the dispersed impurity level. In the critical region of a singularity in the two-particle vertex, a characteristic frequency scale vanishes (analog of the inverse correlation length in standard phase transition). We use this critical scale and separate small (much smaller than the modulus of its logarithm) and large scales. We then replace regular functions (no critical long-range fluctuations) by constants and keep dynamical only the singular functions with critical fluctuations. In this way, we do not affect the universal features of the critical behavior. Unlike the classical criticality, we are, however, unable to uniquely separate short- and long-range fluctuations in the strong-coupling limit of correlated electrons. The universal and nonuniversal properties are mixed up there. We hence have to decouple the short- and long-range fluctuations with an additive approximation to make the ansatz of separation of scales consistent. We can do it in several ways. Here, we discuss two of them. In the first one (introduced in Ref. 18), we demand fulfilling of the parquet equations for regular vertices averaged over short-range fluctuations to obtain constants. This is a mean-field-type approximation that can be applied in the whole region of the input parameters also beyond the critical region of the Bethe-Salpeter equation. It is a fully consistent approximation in the Fermi-liquid regime. Another more accurate way of decoupling short- and long-range fluctuations introduced in this paper is to systematically use the dominant small energy scale shaping the singularity in the vertex function to reduce the frequency dependence of regular functions. The latter approach is more precise as regards the critical behavior but less flexible as regards applicability outside the critical region.

By studying the Kondo behavior in SIAM, we distinguish its two different aspects. First, we introduce a small dimensionless scale connected with a singularity in the two-particle vertex that we call the Kondo scale. From this scale, we derive the Kondo temperature as a cutoff screening the actual singularity that cannot be reached in impurity models. Next, we analyze the behavior of one-electron functions in the Kondo limit, i.e., with a quasidivergent two-particle vertex. We demonstrate the existence of a narrow Kondo resonance peak near the Fermi energy for small deviations from the symmetric situation. We calculate the position of the Kondo peak and estimate its width. We also discuss the existence of the satellite Hubbard bands in the strong-coupling limit.

It is more elaborate to study asymmetric situations in impurity models than the symmetric case. We must introduce an effective chemical potential controlling the occupation of the impurity level. To guarantee consistency of approximations, the chemical potential must be determined self-consistently from the actual filling of the impurity level. It means that independently of the form of one-electron propagators we use in the approximate treatment, we have to calculate impurity filling from the full spectral function with the self-energy obtained in the parquet approximation. We hence

must achieve a static one-particle self-consistency. Only in this way can we avoid spurious (Hartree-type) transitions in the strong-coupling regime.

The paper is organized as follows. In Sec. II, we introduce the parquet equations for impurity models. The simplifications of the parquet equations in the critical region of a singularity in the Bethe-Salpeter equations are discussed in Sec. III. Two-particle functions in the Kondo regime are calculated in Sec. IV and the one-particle functions in Sec. V.

II. PARQUET EQUATIONS FOR IMPURITY MODELS

We start our investigation with the Hamiltonian of SIAM that reads as

$$\hat{H} = \sum_{\mathbf{k}\sigma} \epsilon(\mathbf{k}) c_{\mathbf{k}\sigma}^\dagger c_{\mathbf{k}\sigma} + E_d \sum_{\sigma} d_{\sigma}^\dagger d_{\sigma} + \sum_{\mathbf{k}\sigma} (V_{\mathbf{k}} d_{\sigma}^\dagger c_{\mathbf{k}\sigma} + V_{\mathbf{k}}^* c_{\mathbf{k}\sigma}^\dagger d_{\sigma}) + U \hat{n}_{\uparrow}^d \hat{n}_{\downarrow}^d. \quad (1)$$

We denoted $\hat{n}_{\sigma}^d = d_{\sigma}^\dagger d_{\sigma}$. When calculating the grand potential and thermodynamic properties of the impurity site, we can explicitly integrate over the degrees of freedom of the delocalized electrons. To this purpose, we standardly replace the local part of the propagator of the conduction electrons by a constant $\Delta(\epsilon) = \pi \sum_{\mathbf{k}} |V_{\mathbf{k}}|^2 \delta[\epsilon - \epsilon(\mathbf{k})] \doteq \Delta$, the value of which we set as the energy unit. With this simplification, we expand all dynamical and thermodynamic quantities in powers of the interaction strength U and rearrange appropriately the resulting series.

The principal idea of the parquet approach is to derive the self-energy and other thermodynamic and spectral properties via a two-particle vertex Γ . This vertex is standardly represented via Bethe-Salpeter equations. The Bethe-Salpeter equations express the full two-particle vertex by means of irreducible ones that can be generically represented as¹⁹

$$\Gamma = \Lambda^{\alpha} + [\Lambda^{\alpha} G G]_{\alpha} \star \Gamma, \quad (2a)$$

where Λ^{α} is the irreducible vertex in channel α , the brackets $[\dots]_{\alpha}$ stand for an appropriate interconnection of internal variables in the chosen scattering channel α , and \star represents summation over intermediate states created during the scattering process. We only use singlet electron-hole and electron-electron scattering channels in our consideration.

The consistency of approaches with more two-particle vertices is guaranteed by the parquet equation that reads as

$$\Gamma = \Lambda^{eh} + \Lambda^{ee} - \mathcal{I}. \quad (2b)$$

We introduced a vertex \mathcal{I} irreducible in both channels that in the parquet approximation is replaced by the bare interaction U . The parquet equation in Eq. (2b) states that the full two-particle vertex is a sum of the irreducible vertices from the electron-hole channel (Λ^{eh}) and from the electron-electron channel (Λ^{ee}), from which the completely irreducible vertex (bare interaction) is subtracted. Equation (2b) is used in each Bethe-Salpeter equation in Eq. (2a) to exclude the full vertex Γ and to close the approximation for the irreducible vertices Λ^{eh} and Λ^{ee} . In the impurity case, the dynamical variables in

the vertex functions are Matsubara frequencies. Hence, the explicit form of the parquet equations with the electron-hole

and electron-electron singlet channels reads as

$$\Lambda_{\uparrow\downarrow}^{ee}(i\omega_n, i\omega_{n'}, i\nu_m) = \mathcal{I}_{\uparrow\downarrow}^{eh}(i\omega_n, i\omega_{n'}, i\nu_m) - \frac{1}{\beta} \sum_{n''} \Lambda_{\uparrow\downarrow}^{eh}(i\omega_n, i\omega_{n''}, i\nu_m) G_{\uparrow}(i\omega_{n''}) G_{\downarrow}(i\omega_{n''+m}) [\Lambda_{\uparrow\downarrow}^{ee}(i\omega_{n''}, i\omega_{n'}, i\nu_m) + \Lambda_{\uparrow\downarrow}^{eh}(i\omega_{n''}, i\omega_{n'}, i\nu_m) - \mathcal{I}_{\uparrow\downarrow}(i\omega_{n''}, i\omega_{n'}, i\nu_m)] \quad (3a)$$

and

$$\Lambda_{\uparrow\downarrow}^{eh}(i\omega_n, i\omega_{n'}, i\nu_m) = \mathcal{I}_{\uparrow\downarrow}(i\omega_n, i\omega_{n'}, i\nu_m) - \frac{1}{\beta} \sum_{n''} \Lambda_{\uparrow\downarrow}^{ee}(i\omega_n, i\omega_{n''}, i\nu_{m+n'-n''}) G_{\uparrow}(i\omega_{n''}) G_{\downarrow}(i\omega_{n''+m-n''}) [\Lambda_{\uparrow\downarrow}^{ee}(i\omega_{n''}, i\omega_{n'}, i\nu_{m+n-n''}) + \Lambda_{\uparrow\downarrow}^{eh}(i\omega_{n''}, i\omega_{n'}, i\nu_{m+n-n''}) - \mathcal{I}_{\uparrow\downarrow}(i\omega_{n''}, i\omega_{n'}, i\nu_{m+n-n''})]. \quad (3b)$$

These equations form a set of coupled nonlinear integral equations that cannot be solved by available analytic means. Their numerical solution with $\mathcal{I}=U$ is available only for high temperatures²⁰ in the region irrelevant for quantum effects induced by strong electron correlations. Since we do not know the exact form of the completely irreducible vertex \mathcal{I} , we have to resort to approximations anyway in the parquet approach.

III. TWO-PARTICLE CRITICALITY AND SIMPLIFIED PARQUET EQUATIONS

It is not necessary to always know the detailed form of the completely irreducible vertex \mathcal{I} . It is true, in particular, in the critical region of a two-particle singularity from Bethe-Salpeter equations, where we are interested in universal features of its critical behavior. If the completely irreducible vertex is a regular function (no critical three and higher multiparticle scatterings), it is reasonable to replace it with the bare interaction, which is standardly done in the parquet approximation. It is then futile to try to solve the parquet equations with tremendous effort in regions where no significant deviations from Fermi liquid or gas are present. The principal area of application of the parquet approach should be in the low-temperature strong-coupling region where the standard weak-coupling schemes fail.

The critical region of a singularity in one of the Bethe-Salpeter equations is the situation where the difference between the parquet theory and other weak-coupling schemes becomes significant. Parquet equations, due to their nonlinear character, introduce a two-particle self-consistency enabling to properly handle the two-particle critical behavior. In particular, the two-particle self-consistency effectively suppresses spurious nonphysical (nonintegrable) singularities in two-particle susceptibilities of one-particle approximations. That is why we try to solve the parquet equations, at least in an approximate way, in the critical region of a singularity in Bethe-Salpeter equations. Fortunately, singularities with divergent vertex functions offer a natural way of simplification of the parquet equations. This simplification is

a separation of long-range fluctuations of divergent quantities from the short-range ones of regular functions. In the critical region of a singular vertex, we then treat finite differences in regular functions as negligible with respect to macroscopic changes shaping the singular behavior.

To make the simplification of the parquet equations effective, we must rearrange the weak-coupling expansion in such a way that we first reach the critical region of a singularity in Bethe-Salpeter equations. In SIAM, it is achieved in the random-phase approximation (RPA), that is, the Bethe-Salpeter equation in the electron-hole channel with the bare interaction and the Hartree one-electron propagators. The two-particle vertex in Matsubara frequencies then reads as

$$\Gamma^{RPA}(i\nu_m) = \frac{U}{1 + U\chi_{eh}(i\nu_m)}, \quad (4)$$

where we denoted the dynamical electron-hole bubble with $\chi_{eh}(i\nu_m) = \beta^{-1} \sum_n G_{\uparrow}(i\omega_n) G_{\downarrow}(i\omega_{n+m})$. It is easy to evaluate the electron-hole bubble with the Hartree propagators $G(x+i\nu) = 1/[x - \bar{\mu} + i \operatorname{sgn}(y)(\Delta + |y|)]$ to be

$$\chi_{eh}(z) = - \int_{-\infty}^{\infty} \frac{dx}{\pi} f(x) \left[\frac{1}{x - \bar{\mu} + z + i\Delta} + \frac{1}{x - \bar{\mu} - z + i\Delta} \right] \frac{\Delta}{[(x - \bar{\mu})^2 + \Delta^2]^2}, \quad (5)$$

where $\bar{\mu} = E_d + Un$ is an effective chemical potential measuring deviations from the symmetric case $\bar{\mu} = 0$ and $f(x) = 1/(1 + \exp\{\beta x\})$ is the Fermi function. We used $0 < n < 1$, the actual occupation per spin of the impurity level. Since the static value $\chi_{eh} = \chi_{eh}(0) < 0$, we choose a finite interaction strength U and a very low (zero) temperature T so that we are very close to the singularity in vertex Γ^{RPA} with $0 < 1 + U\chi_{eh} \ll 1$. We now rearrange the expansion beyond RPA in such way that we remain in the critical region of this singularity all the time. We then replace the interaction strength U as an expansion parameter by a new small scale $a = 1 + U\chi_{eh}$. We keep this scale fixed during summation of

diagrams and use it to separate large (relevant) from small (irrelevant) quantities. We will discuss ways how we can use the existence of a small (large) scale to simplify the parquet equations. In fact, we will see that it is not the scale a itself but rather $1/|\ln a|$ that is taken as a small parameter in the expansion beyond RPA in the critical region of the electron-hole vertex. By the parquet equations, we effectively replace the direct summation of diagrams beyond RPA and their renormalization in the critical region of the singularity in the Bethe-Salpeter equation from the electron-hole channel. In analogy with classical criticality, RPA corresponds to a static mean-field approximation and the parquet approach to renormalization-group dynamical corrections to the mean-field critical behavior.

A. Finite temperatures: Mean-field approximation

By solving the parquet equations in the critical region of a Bethe-Salpeter equation, we assume that no other critical point emerges beyond that found in the one-channel (mean-field) approximation. The singularity in SIAM emerges in the electron-hole scattering channel and, hence, the irreducible vertex from the electron-electron channel $\Lambda_{\uparrow\downarrow}^{ee}(i\omega_n, i\omega_{n'}, i\nu_m)$ is singular in the variable $i\nu_m=0$. As no other critical scattering appears in the model, the irreducible vertex from the electron-hole channel $\Lambda_{\uparrow\downarrow}^{eh}(i\omega_n, i\omega_{n'}, i\nu_m)$ remains regular. We now neglect all finite differences in regular functions and replace Λ^{eh} with a constant, an effective interaction \bar{U} . Inserting this ansatz in Eq. (3a), we obtain

$$\Lambda_{\uparrow\downarrow}^{ee}(i\omega_n, i\omega_{n'}; i\nu_m) = U - \frac{\bar{U}^2 \chi_{eh}(i\nu_m)}{1 + \bar{U} \chi_{eh}(i\nu_m)}. \quad (6a)$$

Being in the critical region where the denominator on the right-hand side of Eqs. (6a) and (6b) is very small, we can neglect the contribution to Λ^{ee} from the bare interaction and take into consideration only the low-frequency singular part of this vertex,

$$\Lambda_{\uparrow\downarrow}^{sing}(i\nu_m) = - \frac{\bar{U}^2 \chi_{eh}(i\nu_m)}{1 + \bar{U} \chi_{eh}(i\nu_m)}. \quad (6b)$$

Neglecting finite differences due to the frequency dependence of the regular vertex Λ^{eh} , we have won a simplified frequency dependence of the singular vertex in the form of the RPA vertex Γ^{RPA} from Eq. (4). This simple form enables us to analytically control the critical behavior of the singular vertex Λ^{ee} .

We now insert the derived singular part of the irreducible vertex from the electron-electron channel into Eq. (3b) and obtain

$$\begin{aligned} \bar{U} = U - \frac{1}{\beta} \sum_{n''} \Lambda^{sing}(i\nu_{m+n''-n''}) G_{\uparrow}(i\omega_{n''}) G_{\downarrow}(i\omega_{n+n''+m-n''}) [\bar{U} \\ + \Lambda^{sing}(i\nu_{m+n-n''}) - U]. \end{aligned} \quad (7)$$

This equation is evidently inconsistent, since its right-hand side is frequency dependent. We neglected finite differences in the regular electron-hole irreducible vertex on the left-

hand side of Eq. (7). We must do the same on the right-hand side as well. It contains, however, singular functions. We hence cannot demand equality of both sides for a specifically chosen Matsubara frequency. To make our simplifying ansatz consistent, we have to first regularize the right-hand side of Eq. (7) and grant equality only in a mean. To achieve consistency, we multiply both sides with $G_{\uparrow}(i\omega_n) G_{\downarrow}(i\omega_{m-n})$ and $G_{\uparrow}(i\omega_{n'}) G_{\downarrow}(i\omega_{m-n'})$ and sum over fermionic Matsubara frequencies $i\omega_n$ and $i\omega_{n'}$. We further set $m=0$ to keep the effective interaction real. Since the low-frequency contributions are the most relevant ones, we obtain

$$\bar{U} \chi_{ee} = U \chi_{ee} - \frac{\langle G_{\uparrow} G_{\downarrow} L_{\uparrow\downarrow}^2 \rangle}{\chi_{ee} + \langle G_{\uparrow} G_{\downarrow} L_{\uparrow\downarrow} \rangle}, \quad (8)$$

where $\chi_{ee} = \beta^{-1} \sum_n G_{\uparrow}(i\omega_n) G_{\downarrow}(i\omega_{-n})$ is the static electron-electron bubble. Further on, we used the notation

$$L_{\uparrow\downarrow}(i\omega_n) = \frac{1}{\beta} \sum_{n'} G_{\uparrow}(i\omega_{n'}) G_{\downarrow}(i\omega_{-n'}) \Lambda_{\uparrow\downarrow}^{sing}(i\nu_{-n-n'}), \quad (9a)$$

$$\langle G_{\uparrow} G_{\downarrow} X \rangle = \frac{1}{\beta} \sum_n G_{\uparrow}(i\omega_n) G_{\downarrow}(i\omega_{-n}) X(i\omega_n). \quad (9b)$$

Equations (6a), (6b), (8), (9a), and (9b) form a closed set of relations determining the static effective interaction \bar{U} and the dynamical vertex $\Lambda^{sing}(i\nu_m)$ as functionals of the one-particle propagators G_{σ} and the bare interaction U . They were derived and justified in the critical region of a singularity in the Bethe-Salpeter equation from the electron-hole channel. That is, the denominator on the right-hand side of Eqs. (6a) and (6b) approaches zero. The form of the defining equations for $\Lambda^{sing}(i\nu_m)$ and \bar{U} enables their application in the whole region of the input parameters. The approximation remains consistent everywhere in the Fermi-liquid regime.

B. Zero temperature: Low-frequency approximation

Separation of large scales (potentially divergent functions) and small scales (regular functions) is incomplete in SIAM. To stay close to the critical point of the singularity in Λ^{sing} , we need to know the value of the effective interaction \bar{U} . We do not need to know, however, the detailed frequency dependence of vertex Λ^{eh} but only its action in the Bethe-Salpeter equation in Eq. (3a). With an effective static interaction, we make the replacement

$$\beta^{-1} \sum_{n''} \Lambda_{\uparrow\downarrow}^{eh}(i\omega_n, i\omega_{n''}; i\nu_m) G_{\uparrow}(i\omega_{n''}) G_{\downarrow}(i\omega_{n''+m}) \Lambda_{\uparrow\downarrow}^{ee}(i\omega_{n''}, i\omega_{n'}; i\nu_m) \rightarrow \bar{U} \chi_{eh}(i\nu_m) \Lambda_{\uparrow\downarrow}^{ee}(i\omega_n, i\omega_{n'}; i\nu_m)$$

in the exact parquet equation. This replacement is qualitatively correct if we treat integrals (sums over Matsubara frequencies) of singular functions as regular ones and as far as the effective interaction \bar{U} remains finite. We will see that in SIAM, it is always the case even in the limit $U \rightarrow \infty$.

Although the critical behavior of the singular vertex Λ^{sing} does not depend on the value of the effective interaction \bar{U} , we need its value to determine the asymptotic behavior when the critical point is approached. We need to determine how fast the small scale,

$$a = 1 + \bar{U} \chi_{eh} \rightarrow 0, \quad (10)$$

approaches zero as a function of the input parameters, in particular, of the bare interaction strength U . It is evident that this result depends on the function dependence $\bar{U}(U)$.

The averaging of Eq. (7) we used in the preceding subsection to reach consistency in the determination of the effective interaction is only one, mean-field way. We can proceed in a more accurate way if we fully utilize the dominance of the low-frequency asymptotics of the singular vertex. We can approximate the singular vertex in the critical region with $a \ll 1$ as

$$\Lambda^{sing}(\omega_+) \doteq \frac{\bar{U}}{a - i\bar{U}\chi' \omega / \pi}, \quad (11)$$

where we denoted $\chi' = i\pi \partial \chi_{eh}(\omega_+) / \partial \omega|_{\omega=0}$ and $\omega_+ = \omega + i0^+$. It is clear that only frequencies of order $a\pi / \bar{U}\chi'$ are relevant in integrals with this singular function. It means that only frequencies of order $a / \bar{U}\chi'$ are relevant in regular functions when integrated with the singular vertex. We hence replace all values of the redundant frequencies in regular functions by zero. This is possible only at zero temperature with a continuous distribution of Matsubara frequencies. The nonsingular electron-hole irreducible vertex $\Lambda^{eh}(i\omega_n, i\omega_{n'}; i\nu_m) = \bar{U}$. Such a static replacement cannot be done, however, in singular functions. Before we can set redundant frequencies to zero in Eq. (7), we multiply both sides either by $G_{\uparrow}(i\omega_n)G_{\downarrow}(i\omega_{m-n})$ or by $G_{\uparrow}(i\omega_{n'})G_{\downarrow}(i\omega_{m-n'})$ and integrate over $i\omega_n$ or $i\omega_{n'}$, respectively. The output is a ‘‘sufficiently’’ regular function with maximally logarithmically divergent terms proportional to $|\ln a|$ where we can already set all external frequencies to zero. We then obtain another equation for the effective interaction,

$$\bar{U} \chi_{ee} = U \chi_{ee} - \frac{L_{\uparrow\downarrow}^2}{1 + L_{\uparrow\downarrow}}, \quad (12)$$

where we denoted $L_{\uparrow\downarrow} = L_{\uparrow\downarrow}(0)$. This approximation is applicable only at zero temperature with the sums over Matsubara frequencies replaced by integrals. In this approximation, however, the singularity in the two-particle vertex is treated

more accurately, since, unlike the preceding construction, we treated logarithmically divergent scales of order $|\ln a|$ more sensitively here. Logarithmic terms may be lost or washed out by additional summation over fermionic Matsubara frequencies used in the preceding subsection. It means that our precision is determined by the largest ‘‘regular’’ scale being now of order $|\ln a|$. There is no such small parameter in the construction with Eq. (8).

We would like to comment at this point on a similarity of the presented construction with the local moment approach of Logan *et al.*¹¹ Both theories use multiple scatterings of electron-hole pairs from the RPA channel to explain the strong-coupling logarithmic scale. They, however, differ in the way the unphysical RPA pole from Eq. (4) is shifted from a finite to an infinite interaction strength. In the parquet approach, we use a two-particle self-consistency between electron-hole and electron-electron scatterings. By the latter, we renormalize the bare interaction strength U to \bar{U} . The renormalized interaction overtakes the control of how the denominator of the two-particle vertex approaches zero. The two-particle bubble χ_{eh} remains untouched. The local moment approach keeps the interaction strength unrenormalized and makes the two-particle bubble interaction dependent. This is achieved by introducing a symmetry breaking parameter $0 \leq m \leq 1$, modulus of a static local magnetic moment. The moment then splits the solution into two spin-dependent components. The value of the magnetic moment is defined from a renormalized Hartree condition and saturates only in the strong-coupling regime $U \rightarrow \infty$. As a consequence, the two-particle bubble for each magnetic solution asymptotically vanishes and the RPA pole is moved to infinity.

IV. KONDO SCALE AND KONDO TEMPERATURE

We now proceed with solving the derived simplified parquet equations for the singular vertex $\Lambda^{sing}(\omega_+)$ and the effective interaction \bar{U} . We resort to the spin-symmetric case $G_{\uparrow} = G_{\downarrow}$ and analyze the solution in the critical region of the singularity with $a = 1 + \bar{U} \chi_{eh} = 1 - \bar{U} \int_{-\infty}^{\infty} d\omega f(\omega) \Im[G_{\pm}(\omega)^2] / \pi \rightarrow 0$. We used the abbreviation $G_{\pm}(\omega) \equiv G(\omega \pm i0^+)$. The new small dimensionless scale a emerging in the critical region of the two-particle vertex is dominant for the determination of the behavior of SIAM in the strong-coupling regime. We call it a Kondo scale, since, as we will demonstrate below, it gives origin to and controls the Kondo strong-coupling asymptotics known from the exact Bethe-ansatz solution.

We first evaluate the dominant contributions from the singular vertex $\Lambda^{sing}(\omega_+)$ to the integral $L_{\uparrow\downarrow}$ in the limit $a \rightarrow 0$. We simultaneously use both reduction schemes, Eqs. (8) and (12), the former for nonzero temperatures and the latter at zero temperature. Using the low-frequency asymptotics [Eq. (11)], we obtain at finite temperatures:

$$L_{\uparrow\downarrow}(z) \doteq \frac{G(z)G(-z)}{\chi'} \int_0^\xi \frac{dx}{\tanh(bx/2)} \frac{x}{a^2 + x^2}, \quad (13a)$$

where we denoted a dimensionless inverse temperature $b = \pi\beta/\bar{U}\chi'$, effective bandwidth $\xi = \bar{U}\chi'D/\pi$, and $\chi' = -4\int_{-\infty}^{\infty} dx f(\Delta x + \bar{\mu})x(x^2+1)^{-3}$. At low temperatures, at which the integral becomes singular and the asymptotic representation in Eq. (13a) holds, we further obtain

$$L_{\uparrow\downarrow}(z) \doteq \frac{G(z)G(-z)}{2\chi'} \left[\ln\left(\frac{b^2}{1+b^2a^2}\right) + \frac{4}{ba} \arctan\left(\frac{1}{ba}\right) \right]. \quad (13b)$$

The leading singular contribution to the integral L at zero temperature comes out rather simply as

$$L_{\uparrow\downarrow}(z) \doteq \frac{G(z)G(-z)}{\pi^2\rho_0^2} |\ln a|, \quad (13c)$$

where $\rho_0 = \Delta/\pi(\Delta^2 + \bar{\mu}^2)$ is the density of states at the Fermi energy.

The Parquet equations in Eqs. (6a), (6b), and (8) do not allow for a solution with a critical point ($a=0$) at a finite temperature, that is, with $ba=0$. The critical point can only be asymptotically approached when the temperature approaches zero. Actually, the critical behavior saturates when the product ba becomes of order unity. In the asymptotic limit $b \rightarrow \infty$, this condition defines a temperature at which the static two-particle vertex function asymptotically approaches its maximal value. In the Kondo regime, below this saturation temperature (called Kondo temperature), physical quantities are saturated and the Kondo temperature overtakes the role of the temperature scale. Using the low-temperature asymptotics from Eq. (13b) together with the condition $ba=1$ in Eq. (8), we obtain the following expression for the Kondo temperature:

$$k_B T_K = \frac{\pi|\chi_{eh}|}{\chi'} \exp\left\{ -\frac{\chi' \chi_{ee}}{|\chi_{eh}|} (U|\chi_{eh}| - 1) \frac{\langle(GG)_{ee}^2\rangle}{\langle(GG)_{ee}^3\rangle} \right\}, \quad (14a)$$

where we denoted $\langle(GG)_{ee}^n\rangle = -\pi^{-1} \int_{-\infty}^{\infty} dx f(x) \mathfrak{I}\{[G_+(x)G_-(-x)]^n\}$. The Kondo regime sets in only asymptotically in the limit $U|\chi_{eh}(0)| \rightarrow \infty$. The genuine strong-coupling regime in SIAM sets in already for $U|\chi_{eh}(0)| > 1$. This regime is not reached by simpler weak-coupling approximations such as RPA or FLEX, where $U|\chi_{eh}(0)| < 1$ always. Notice that the Kondo temperature cannot be defined unambiguously and Eq. (14a) is valid as order of magnitude only.

By using Eq. (12), we cannot determine the Kondo temperature directly, since it is applicable only at zero temperature. We can nevertheless determine the Kondo scale a as a function of the bare interaction strength. By inserting the asymptotic result from Eq. (13c) into Eq. (12), we obtain an equation for $|\ln a|$. From it, we find a solution for the Kondo scale,

$$a = \exp\left\{ -\frac{\chi_{ee}}{|\chi_{eh}|} (U|\chi_{eh}| - 1) \right\}. \quad (14b)$$

Expressions (14a) and (14b) for the Kondo temperature and the Kondo scale were derived for an arbitrary form of the one-electron propagators. The only assumption was that the electron-hole bubble $\chi_{eh}(z)$ is analytic at $z=0$. We argued in Ref. 18 that the Hartree one-electron propagators deliver the best results in SIAM on both small and large energy scales. Any *dynamical* one-electron self-consistency negatively interferes in the control of the two-particle singularity in the Bethe-Salpeter equation won by the parquet approximation. In particular, the electron-hole bubble $\chi_{eh} \rightarrow 0$ with $U \rightarrow \infty$ when calculated with the fully renormalized one-electron propagators, which forces the effective interaction to diverge. Our simplifying scheme was justified for finite effective interaction $\bar{U} < \infty$. The parquet approximation for the vertex functions with $\mathcal{I}=U$ corresponds to a Hartree approximation on the one-particle level. Going beyond Hartree propagators in the parquet scheme demands to renormalize adequately the completely irreducible vertex \mathcal{I} to keep the approximation consistent. The only peremptory one-particle self-consistency is the static one, where the effective chemical potential $\bar{\mu}$ is calculated from the fully renormalized one-electron propagator.

We hence use the Hartree propagators in our parquet approximation to evaluate explicitly the two-particle functions in Eqs. (14a) and (14b). In the low-temperature limit, the dominant contribution to the Kondo temperature comes from the zero-temperature values of the functions on the right-hand side of Eq. (14a). At zero temperature, the two-particle bubbles read as

$$\chi_{eh} = -\frac{1}{\pi} \frac{\Delta}{\Delta^2 + \bar{\mu}^2}, \quad (15a)$$

$$\chi_{ee} = \frac{1}{2\pi\bar{\mu}} \left[\frac{\pi}{2} + \arctan\left(\frac{\bar{\mu}^2 - \Delta^2}{2\Delta\bar{\mu}}\right) \right], \quad (15b)$$

$$\chi' = \frac{\Delta^4}{(\Delta^2 + \bar{\mu}^2)^2}. \quad (15c)$$

Further on, we obtain

$$\langle(GG)_{ee}^2\rangle = \frac{1}{4\pi\bar{\mu}^3} \left[\frac{\pi}{2} + \arctan\left(\frac{\bar{\mu}^2 - \Delta^2}{2\Delta\bar{\mu}}\right) - \frac{2\Delta\bar{\mu}}{\Delta^2 + \bar{\mu}^2} \right], \quad (16a)$$

$$\langle(GG)_{ee}^3\rangle = \frac{1}{16\pi\bar{\mu}^5} \left[\frac{3\pi}{2} + 3 \arctan\left(\frac{\bar{\mu}^2 - \Delta^2}{2\Delta\bar{\mu}}\right) - \frac{2\Delta\bar{\mu}(3\Delta^2 + 5\bar{\mu}^2)}{(\Delta^2 + \bar{\mu}^2)^2} \right]. \quad (16b)$$

The effective interaction in the Kondo regime reads as $\bar{U} = \pi(1-a)(\bar{\mu}^2 + \Delta^2)/\Delta$.

With the above representation, we obtain an explicit dependence of the Kondo temperature on the interaction strength U and the effective chemical potential $\bar{\mu}$. We explicitly mention only two important limits. First, in the symmetric case $\bar{\mu}=0$, we have

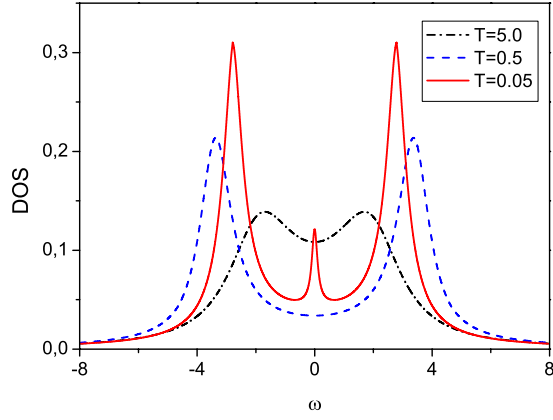


FIG. 1. (Color online) Density of states for $U=4$ and various temperatures demonstrating formation of the Kondo resonance at the Fermi energy for the symmetric case. The zero-temperature value of the density of states is due to the Friedel sum rule $1/\pi$.

$$k_B T_K \doteq \Delta \exp\left\{-\frac{5}{3}[U\rho_0 - 1]\right\}. \quad (17a)$$

The Kondo temperature is determined by the Kondo dimensionless scale derived in Ref. 18.

The other limit with a simple representation of the Kondo temperature is an almost empty impurity level where $\bar{\mu} \gg \Delta$. In this case, we obtain

$$k_B T_K \doteq \frac{\bar{\mu}^2}{\Delta} \exp\left\{-\frac{2\pi\Delta}{3\bar{\mu}}\left(\frac{U\Delta}{\pi\bar{\mu}^2} - 1\right)\right\}, \quad (17b)$$

where $\bar{\mu} = E_d + Un$. For $\bar{\mu} \gg \Delta$, we explicitly have $\bar{\mu} = E_d(1 - \sqrt{1 + 4U\Delta/\pi E_d^2})/2$ and $n \sim \Delta/\pi\bar{\mu}$, from which we get $\bar{\mu} \sim |E_d|$ and $E_d^2 \sim U\Delta$. We see that the strong-coupling regime $U\Delta > \pi E_d^2$ sets in also for an almost empty impurity level, but the Kondo temperature is no longer exponentially small.

The Kondo scale calculated from Eq. (21) with Hartree propagators reads as

$$a = \exp\left\{-\frac{\pi/2 + \arctan\left(\frac{\bar{\mu}^2 - \Delta^2}{2\bar{\mu}\Delta}\right)}{2\bar{\mu}\Delta} \left[\frac{U}{\pi}\Delta - \Delta^2 - \bar{\mu}^2\right]\right\}. \quad (18a)$$

In the symmetric case and for an almost empty impurity level, it reduces to

$$a = \exp\{- (U\rho_0 - 1)\} \quad (18b)$$

and

$$a = \exp\left\{-\frac{\pi}{2|E_d|\Delta}(U\Delta - E_d^2)\right\}, \quad (18c)$$

respectively. Using further the solution for E_d in the limit $n \rightarrow 0$, we obtain an asymptotic dependence $a \sim \exp\{-\frac{\alpha\pi}{2\Delta}|E_d|\}$ or $a \sim \exp\{-\alpha'\sqrt{\frac{U}{\Delta}}\}$ for $U \rightarrow \infty$. The Kondo regime sets in for an almost empty impurity level if $Un^2 > \pi^2\Delta$.

Both expressions (17a) and (18b) for the Kondo temperature in the symmetric case qualitatively agree (in universal

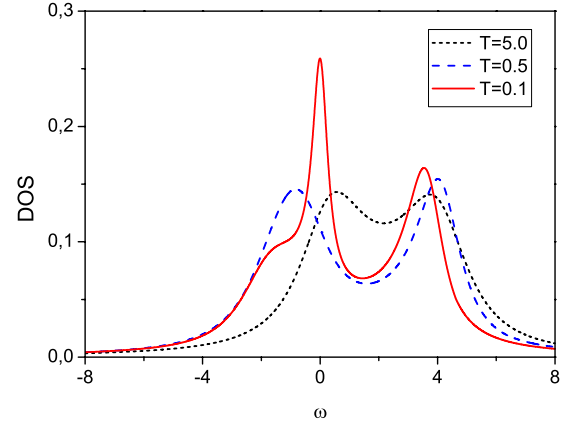


FIG. 2. (Color online) Temperature dependence of the density of states for a partial occupation of the impurity level $n=0.4$ and $U=4$.

features) with the exact formula $k_B T_K \doteq \sqrt{U\Delta/2} \exp\{\pi E_d(E_d + U)/2\Delta U\}$ known from the s - d exchange Hamiltonian asymptotically reached in the limit $U \rightarrow \infty$ of SIAM.²¹ The Kondo temperature for an almost empty impurity level [Eq. (17b)] deviates in the dependence on E_d from the exact result. The two asymptotic results were, however, derived under different conditions. The former representation was obtained for a fixed $\bar{\mu} \gg \Delta$ while the latter for a fixed E_d constrained to $E_d \ll -\Delta$ and $E_d + U \gg \Delta$.²² The Kondo scale from Eq. (18c) improves upon this imperfection in the asymmetric situation of the approximate scheme based on Eq. (8). It qualitatively reproduces well the exact result with the exponent linearly proportional to the position of the impurity level E_d . As expected, the zero-temperature, low-frequency approximation on the effective interaction \bar{U} [Eq. (12)] reproduces better the dependence of the Kondo scale on the interaction strength and, in particular, on the position of the impurity level and the impurity-level occupation.

V. SELF-ENERGY: KONDO RESONANCE AND HUBBARD SATELLITE BANDS

We defined the Kondo temperature and the Kondo scale from a critical behavior of the two-particle vertex near a singularity in the electron-hole correlation function. The one-electron propagators were used as input parameters for the two-particle vertices. In this situation with one-electron propagators chosen independently of the two-particle ones, we cannot interpret the two-particle functions we use as the actual physical quantities they diagrammatically stand for. We have to conform with conservation laws of consistent theories. To make the approximation thermodynamically consistent, we have to introduce the self-energy as a functional of the two-particle vertex. The physical quantities in conserving theories are then derived from the self-energy via appropriate (functional) derivatives.

We use the Schwinger-Dyson equation to relate the self-energy with the two-particle vertex.¹⁸ In our case of the simplified parquet equations, it reduces to

$$\Sigma_{\sigma}(i\omega_n) = \frac{U}{\beta} \sum_{n'} \frac{G_{-\sigma}(i\omega_{n'})}{1 + \bar{U}\chi_{eh}(i\omega_{n'} - i\omega_n)}. \quad (19)$$

In the spin-symmetric case and in the Kondo regime (critical region of the singularity in the two-particle vertex), we again use the low-frequency expansion of the denominator in the

analytically continued version of Eq. (19). We further employ the electron-hole symmetry of the Hartree propagators $G(i\omega_n - \bar{\mu}) = -G(-i\omega_n + \bar{\mu})$ to guarantee analytic properties also in approximate numerical evaluations of the self-energy. After analytic continuation, we explicitly obtain the following expressions for the real and imaginary parts of the self-energy:

$$\Re\Sigma(y) = \frac{U|\chi_{eh}(0)|}{2\pi(1-a)\chi'} \int_{-\infty}^{\infty} \frac{dx}{(x+y-\bar{\mu})^2 + 1} \frac{1}{x^2 + \tilde{a}^2} \left\{ \frac{x(x+y-\bar{\mu})}{\tanh(\beta x/2)} - \tilde{a} \tanh[\beta(x+y)/2] \right\}, \quad (20a)$$

$$\Im\Sigma(y) = -\frac{U|\chi_{eh}(0)|}{2\pi(1-a)\chi'} \int_{-\infty}^{\infty} \frac{dx}{(x+y-\bar{\mu})^2 + 1} \frac{x}{x^2 + \tilde{a}^2} \left\{ \frac{1}{\tanh(\beta x/2)} - \tanh[\beta(x+y)/2] \right\}, \quad (20b)$$

where we set $\Delta=1$ and denoted $\tilde{a}=a\pi|\chi_{eh}(0)|/(1-a)\chi'$. The representation in Eqs. (20a) and (20b) is meaningful for $0 \leq a \leq 1$, but it is justified in the asymptotic limits $\beta \rightarrow \infty$ and $\beta a \sim 1$. The physics in the Kondo regime of SIAM, including the effective chemical potential $\bar{\mu}$, in this approximation is determined from the self-energy in Eqs. (20a) and (20b) and its dependence on external sources entering the theory via the Hartree propagators. The approximation in Eqs. (20a) and (20b) obeys the necessary symmetry relations and sum rules. It defines a Fermi liquid with the imaginary part of the self-energy proportional to the square of the frequency distance from the Fermi level.

For a numerical solution (not deep in the Kondo regime), it is straightforward to iterate Eqs. (6a) and (6b) with either Eq. (8) or (12) and use their solution in Eq. (19) to determine dynamical and thermodynamic properties of SIAM. The numerical effort is comparable with the numerical solution of FLEX-type approximations. Even better, by fixing the Kondo scale a , instead of the bare interaction U , we succeeded in improving significantly upon the numerical stability of the existing numerical schemes for these types of approximations.

Figure 1 shows the temperature dependence of the spectral density for $U=4$ and half-filling. When the temperature decreases, quasiparticle states are first expelled from the Fermi energy to satellite peaks. However, at temperatures of order of the Kondo one, a new resonance around the Fermi energy starts to develop, so that the singularity in the vertex function gets screened. This scenario takes place at arbitrary filling, but the exponentially narrow Kondo resonance realizes practically only for fillings close to the symmetric case (Fig. 2). Farther apart from the half-filled case, the Kondo temperature increases and the quasiparticle peak broadens and gradually merges with the lower satellite band (Fig. 3). The numerical results for the symmetric case are in good qualitative agreement with the behavior obtained by NRG in Ref. 15. There is more weight in the satellite bands in the parquet solution than in NRG. A more significant difference can be observed when the charge symmetry is lifted. The

Kondo peak in the parquet solution does not stick to the Fermi surface and moves away with increasing asymmetry toward a Hubbard satellite band. This phenomenon is not observed in NRG calculations of Ref. 15. We should realize that there is no sum rule that would pin the density of states at the Fermi energy to a fixed value away from the symmetric case. Not only the height but also the position of the resonant peak varies with the impurity-level filling.

We used Eq. (11) for the determination of the effective interaction \bar{U} in the calculations of the self-energy and the spectral function. The differences in the results obtained with the other approximate decoupling of the parquet equations in Eq. (12) are not dramatic. The results are qualitatively the same with minor quantitative deviations, as demonstrated in Fig. 4. In the symmetric situation, the distance between the satellite peaks is smaller and the central peak is slightly broader when Eq. (12) is used.

Critical behavior of the two-particle vertex in the Kondo regime ($a \ll 1$) allows one to analytically assess the self-

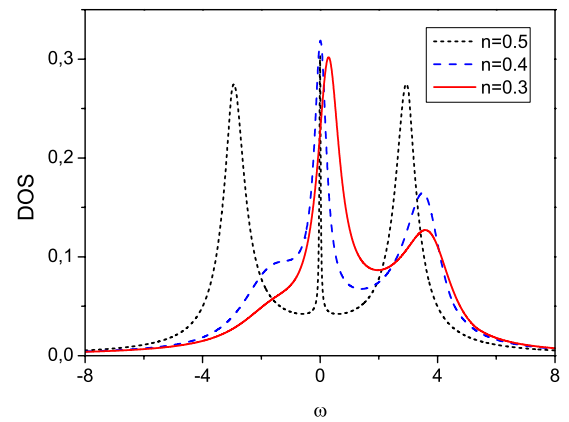


FIG. 3. (Color online) Dependence of the Kondo resonant peak on filling of the impurity level for $U=4$ and $T=0$. Merging of the quasiparticle peak with the lower Hubbard band for lower fillings is apparent.

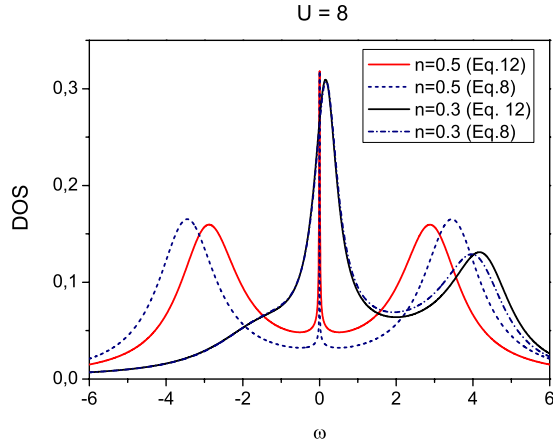


FIG. 4. (Color online) Spectral function calculated with the effective interactions from Eqs. (8) and (12) for $U=8$ and $T=0$. The two approximate schemes do not significantly differ at any filling except for a narrow asymptotic critical region of asymmetric models.

energy and the resulting spectral function. Using the fact that $a \rightarrow 0$ in Eqs. (20a) and (20b), we obtain the following representation for the leading asymptotic behavior of the self-energy at zero temperature:

$$\Re \Sigma(\omega_+) = \frac{U \ln \left[1 + \frac{\bar{U}^2 \pi^2 \rho_0^4 \xi^2}{a^2} \right]}{2\bar{U} \pi^2 \rho_0^2} \Re \mathcal{G}(\omega_+) + \frac{U \arctan \left(\frac{\bar{U} \pi \rho_0^2 \omega}{a} \right)}{\bar{U} \pi^2 \rho_0^2} \Im \mathcal{G}(\omega_+), \quad (21a)$$

$$\Im \Sigma(\omega_+) = \frac{U \ln \left[1 + \frac{\bar{U}^2 \pi^2 \rho_0^4 \omega^2}{a^2} \right]}{2\bar{U} \pi^2 \rho_0^2} \Im \mathcal{G}(\omega_+). \quad (21b)$$

The representation in Eqs. (21a) and (21b) is quite general and holds in the Kondo regime for any form of the one-electron propagator \mathcal{G} used in the parquet approximation. That is, with this representation, we can analyse any dispersion relation or approximate form of the one-electron propagators used in the Schwinger-Dyson equation [Eq. (19)]. Most importantly, we can assess the width of the Kondo resonance near the Fermi energy and decide about the existence of the satellite upper and lower Hubbard bands. In Fig. 5, we compared the real part of the self-energy calculated with the full representation [Eqs. (20a) and (20b)] and the asymptotic form [Eqs. (21a) and (21b)]. We can see that there are no relevant (qualitative) differences in the results and the agreement is almost perfect in the critical region and for small energies near the Fermi energy. The asymptotic formula should hold in the critical region with $a \ll 1$ and, hence, the deeper in the critical (Kondo) region we are, the better the agreement becomes.

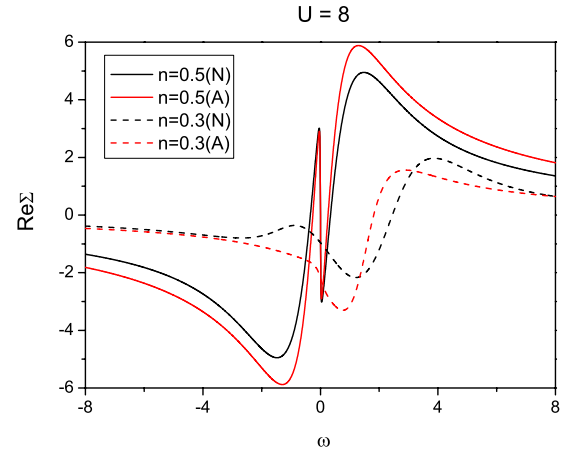


FIG. 5. (Color online) Real part of the self-energy from the numerical solution (N) and the asymptotic form from Eqs. (21a) and (21b) (A) at zero temperature and two fillings. The critical behavior is more pronounced in the asymptotic solution.

We already proved in Ref. 18 that one-particle self-consistent approximations with fully renormalized one-electron propagators smear out the satellite Hubbard bands. On the other hand, numerical calculations clearly demonstrate that the approximation with the Hartree one-electron propagators leads to satellite bands. With the asymptotic formulas (21a) and (21b), we can even prove it and determine the positions of these bands.

We use Hartree propagators in Eqs. (21a) and (21b). The effective chemical potential $\bar{\mu}$ is determined from the actual occupation of the impurity level. We first estimate the position of the Kondo resonance peak, that is, maximum of the spectral function very close to the Fermi energy, within a frequency region of order of the Kondo scale. We determine the center of the Kondo peak from vanishing of the imaginary part of the one-electron propagator. The maximum of the spectral function at the Fermi energy is guaranteed by the Friedel sum rule only at half-filling. By using the Hartree propagators on the right-hand side of Eqs. (21a) and (21b) for the self-energy, we obtain a solution for $\partial \Im[\omega - \bar{\mu} + i\Delta - \Sigma(\omega_+)]^{-1} / \partial \omega = 0$ in the form

$$\tilde{x} = \frac{2U(\pi + U \ln \sqrt{1 + \tilde{x}^2})[\arctan(\tilde{x}) + \bar{\mu} \ln a]}{U^2[\arctan(\tilde{x}) + \bar{\mu} \ln a]^2 - (\pi + U \ln \sqrt{1 + \tilde{x}^2})^2}, \quad (22)$$

where we denoted $\tilde{x} = \omega/a(1 + \bar{\mu}^2)$ and assumed that it is of order unity. In the symmetric case ($\bar{\mu} = 0$), we have the trivial solution $x=0$. The position of the Kondo resonance peak moves off the Fermi energy in the opposite direction given by the effective chemical potential $\bar{\mu} = E_d + Un$. For small values of $\bar{\mu}$, we explicitly obtain

$$\omega_0 = -\frac{2U\bar{\mu}a \ln a}{\pi}. \quad (23)$$

The maximum of the spectral function for larger effective chemical potentials $\bar{\mu} \gg \pi/|\ln a|$ eventually moves out from a region of order of the Kondo scale around the Fermi energy.

The width of the Kondo resonance can be estimated from the distance between the opposite points of steepest descent of the spectral function around the peak near the Fermi energy. They can be obtained as points where the derivative of the real part of the one-electron propagator vanishes. It happens for

$$\tilde{x} = \frac{(\pi + U \ln \sqrt{1 + \tilde{x}^2})^2 - U^2 [\arctan(\tilde{x}) + \bar{\mu} |\ln a|]^2}{2U [\arctan(\tilde{x}) + \bar{\mu} |\ln a|] (\pi + U \ln \sqrt{1 + \tilde{x}^2})}. \quad (24)$$

For small effective chemical potentials ($\bar{\mu} \ll \pi/2 |\ln a|$), Eq. (24) has two solutions $\tilde{x} \sim 1$. The Kondo peak is then well formed. It broadens with increasing the effective chemical potential. Above the critical value $\bar{\mu} = \pi/2 |\ln a|$, one of the solutions is pushed to (minus) infinity and the Kondo peak dissolves in the bulk of other states.

The positions of the centers of the satellite Hubbard bands can be determined from vanishing of the imaginary part of the full one-particle propagator. We have two solutions apart from the Fermi energy. The centers of the satellite peaks are determined from a solution proportional to the logarithm of the Kondo scale $|\ln a|$. We obtain the following solution for the Hartree propagators in SIAM:

$$\Omega_{\pm} = \bar{\mu} \pm \sqrt{\frac{U |\ln a|}{\bar{U} \pi^2 \rho_0^2}} = \bar{\mu} \pm \frac{\sqrt{U \chi_{ee} (U |\chi_{eh}| - 1)}}{\pi |\chi_{eh}|}, \quad (25)$$

where the two-particle bubbles χ_{ee} and χ_{eh} are determined from Eqs. (15a)–(15c). In the symmetric case, we have $\Omega_{\pm} = \pm U/\pi$. This result deviates from the atomic limit values $\Omega_{\pm} = \pm U/2$ that can be generally deduced from the exact second moment of the spectral function in the strong-coupling regime.²³ Neither the atomic limit nor the second moment of the spectral function is exactly reproduced in the presented simplified parquet approach. This is, however, not surprising, since our approximation is justified for small energy scales where the contributions from the singular part of the vertex function are dominant. Away from the half-filled impurity level, the distance between the satellite peaks increases with the square root of the effective chemical potential $\bar{\mu}$. Equation (25) also tells us that the Hubbard satellite bands may exist only in the strong-coupling regime defined as $U |\chi_{eh}| > 1$. The Kondo regime sets in even later for $U |\chi_{eh}| \gg 1$.

VI. CONCLUSIONS

We studied the single-impurity Anderson model in the strong-coupling regime with the aim of developing a reliable and analytically controllable approximation in this regime. We succeeded in simplifying the parquet equations to a manageable form without losing consistency and fundamental characteristics of the Fermi-liquid regime for arbitrary fillings of the impurity level. We showed that the derived simplified parquet equations for two-particle irreducible vertices in the electron-hole (Λ^{eh}) and electron-electron (Λ^{ee}) singlet channels result from a resummation of the diagrammatic perturbation expansion in the critical region of a singularity in the two-particle vertex. Such a singularity emerges in SIAM

due to multiple electron-hole scatterings. The resummation of the perturbation expansion proceeds so that the critical region is reached first within RPA. Diagrammatic contributions beyond RPA are then summed to not be driven out of the critical region of the two-particle vertex. The singularity in the two-particle vertex is controlled by a vanishing scale. This new scale replaces the interaction strength in the perturbation expansion beyond RPA and is used to select relevant contributions in the critical regime.

The principal assumption for rearranging the diagrammatic expansion in a two-particle criticality is to explicitly sum and control two-particle contributions. We distinguish two basic classes of two-particle functions: singular and regular. The former diverge with vanishing of the critical scale and the latter remain finite. Logarithmically divergent functions (integrals over the singular functions) are treated as (marginally) regular ones. The critical scale enables us to neglect finite differences in the regular two-particle functions and replace them with constants. Only the potentially divergent functions are kept dynamical in the two-particle criticality. Even more, only the singular low-frequency asymptotics matters in the critical region.

It is clear that contributions beyond RPA must be summed in a self-consistent way to make the perturbation theory of SIAM singularity-free for any finite interaction strength. The parquet equations provide us with the necessary two-particle self-consistency. We presented two ways of how to simplify the parquet equations in the critical region of the singularity in the electron-hole channel. They differ in the way we suppress the frequency dependence of regular functions. This ambiguity, however, influences only nonuniversal critical properties. In the first construction, we replaced the regular vertices with their specific averaged values. In the second one, we used the fact that only frequencies of order of the vanishing critical scale remain important. In both cases, we reached a set of manageable equations determining an effective interaction, replacing the bare one in RPA, and the singular two-particle vertex.

The solution of the simplified parquet equations led to the Kondo behavior in the strong-coupling regime for all fillings of the impurity level. We found that the vanishing critical scale of the two-particle vertex is the one determining the Kondo temperature at which the two-particle vertex saturates and the Kondo temperature overtakes the control of the low-temperature behavior of two-particle vertex and correlation functions. We thus find that the Kondo behavior is a consequence of a critical behavior due to a singularity in the local two-particle vertex induced by frequency fluctuations. The critical point in SIAM is reached only by infinite bare interaction, but the critical region extends deep into the physical domain of its finite values. Unlike the existing (approximate) solutions of SIAM, we clearly demonstrated the two-particle origin of the Kondo behavior. In fact, it is not the density of states on the Fermi surface ρ_0 that controls the Kondo behavior but rather the electron-hole bubble $|\chi_{eh}|$. It is fortunate that for the Lorentzian DOS used here and in the Bethe ansatz, the two numbers coincide.

Finally we investigated one-electron functions in the Kondo regime. We related the two-particle Kondo scale with the width of the quasiparticle peak near the Fermi energy and

found good qualitative agreement with the exact result. We were able to estimate analytically the width of this peak and showed that it is well formed only close to the half-filled case. Farther away from the symmetric situation, the Kondo resonance dissolves in the bulk of other states. We also showed that our parquet approximation not only reproduces correctly the Kondo resonance in the spectral function but is also able to produce the satellite Hubbard bands. We found a criterion for their existence and an estimate for the positions of their centers.

To summarize, we presented a simple analytic approximation producing dynamical properties of SIAM for all interaction strengths and impurity fillings. It correctly reproduces universal features of the low-temperature Kondo behavior and predicts a Kondo resonance peak near the Fermi energy in the strong-coupling regime for small deviations from the electron-hole symmetric case. At intermediate couplings, it is in good quantitative agreement with more laborious numerical renormalization-group calculations. We identified the

Kondo behavior as the critical behavior near a singularity in the electron-hole Bethe-Salpeter equation with balanced electron-hole and electron-electron multiple scatterings. The electron-hole scatterings are needed to reach a singularity in Bethe-Salpeter equations and the electron-electron ones to screen the interparticle interaction. Due to its universality, the approximation can be easily extended to more complex multiorbital or translationally invariant lattice models for a reliable qualitative and quantitative investigation of a transition from weak- to strong-coupling regimes in materials with tangible electron correlations.

ACKNOWLEDGMENTS

This research was carried out within Project No. AVOZ10100520 of the Academy of Sciences of the Czech Republic and supported in part by Grant No. 202/07/0644 of the Grant Agency of the Czech Republic. We thank Matouš Ringel for valuable and inspiring discussions.

*janis@fzu.cz

†august@fzu.cz

¹P. W. Anderson, Phys. Rev. **124**, 41 (1961),.

²J. Kondo, Prog. Theor. Phys. **32**, 37 (1964).

³A. M. Tsvelik and P. B. Wiegmann, Adv. Phys. **32**, 453 (1983).

⁴A. Georges, G. Kotliar, W. Krauth, and M. Rozenberg, Rev. Mod. Phys. **68**, 13 (1996).

⁵K. Yosida and K. Yamada, Suppl. Prog. Theor. Phys. **46**, 439 (1970).

⁶V. Zlatić and B. Horvatić, Phys. Rev. B **28**, 6904 (1983).

⁷N. E. Bickers and D. J. Scalapino, Ann. Phys. (N.Y.) **193**, 206 (1989).

⁸A. C. Hewson, Phys. Rev. Lett. **70**, 4007 (1993).

⁹H. Keiter and J. C. Kimball, Phys. Rev. Lett. **25**, 672 (1970).

¹⁰T. Pruschke and N. Grewe, Z. Phys. B: Condens. Matter **74**, 439 (1989).

¹¹D. E. Logan, M. P. Ewastwood, and M. A. Tusch, J. Phys.: Condens. Matter **10**, 2673 (1998).

¹²R. M. Fye and J. E. Hirsch, Phys. Rev. B **38**, 433 (1988).

¹³K. G. Wilson, Rev. Mod. Phys. **47**, 773 (1975).

¹⁴H. R. Krishna-murthy, J. W. Wilkins, and K. G. Wilson, Phys. Rev. B **21**, 1003 (1980). **21**, 1044 (1980).

¹⁵T. A. Costi, A. C. Hewson, and V. Zlatić, J. Phys.: Condens. Matter **6**, 2519 (1994).

¹⁶R. Bulla, A. C. Hewson, and T. Pruschke, J. Phys.: Condens. Matter **10**, 8365 (1998).

¹⁷A. C. Hewson, *The Kondo Problem to Heavy Fermions* (Cambridge University Press, Cambridge, 1993).

¹⁸V. Janiš and P. Augustinský, Phys. Rev. B **75**, 165108 (2007).

¹⁹V. Janiš, Phys. Rev. B **60**, 11345 (1999).

²⁰C. X. Chen and N. E. Bickers, Solid State Commun. **82**, 311 (1992).

²¹A. M. Tsvelik and P. B. Wiegmann, Phys. Lett. **89A**, 368 (1982).

²²F. D. M. Haldane, Phys. Rev. Lett. **40**, 416 (1978).

²³S. R. White, Phys. Rev. B **44**, 4670 (1991).